HHS Public Access

Author manuscript

Cell. Author manuscript; available in PMC 2015 August 14.

Published in final edited form as:

Cell. 2014 August 14; 158(4): 808–821. doi:10.1016/j.cell.2014.06.025.

State-dependent architecture of thalamic reticular sub-networks

Michael M. Halassa[1,2,*], **Zhe Chen**[1,2], **Ralf D. Wimmer**[1,2], **Philip M. Brunetti**[2], **Shengli Zhao**[3], **Basilis Zikopoulos**[4], **Fan Wang**[3], **Emery N. Brown**[5], and **Matthew A. Wilson**[2]

[1] Neuroscience Institute, New York University Langone Medical Center, NY 10016, USA; Departments of Psychiatry and Neuroscience & Physiology, New York University Langone Medical Center, NY 10016, USA

[2] Picower Institute for Learning and Memory, Massachusetts Institute of Technology, Cambridge, MA 02139, USA

[3] Department of Cell Biology, Duke University, Durham, NC 27710, USA

[4] Department of Health Sciences and Program in Neuroscience, Boston University, Boston MA 02215, USA

[5] Department of Anesthesia, Critical Care and Pain Medicine, Massachusetts General Hospital, Boston, MA, USA; Harvard Medical School, Boston, MA, USA; Department of Brain and Cognitive Sciences, Massachusetts Institute of Technology, Cambridge, MA, USA; Harvard-MIT Division of Health Sciences and Technology, Institute of Medical Engineering and Science, Massachusetts Institute of Technology, Cambridge, MA, USA

Abstract

Behavioral state is known to influence interactions between thalamus and cortex, which are important for sensation, action and cognition. The thalamic reticular nucleus (TRN) is hypothesized to regulate thalamo-cortical transmission, but the underlying functional architecture of this process and its state-dependence are unknown. By combining the first TRN ensemble recording with psychophysics and connectivity-based optogenetic tagging, we find that the TRN is composed of distinct sub-networks. While activity of limbic-projecting TRN neurons correlates with arousal, sensory-projecting neurons participate in spindles and show elevated synchrony by slow waves during sleep. Conversely, sensory-projecting neurons are suppressed by attentional states, demonstrating common microcircuit mechanisms of sensory processing in sleep and attention. Bidirectional manipulation of attentional performance was achieved through optogenetic

* To whom correspondence should be addressed. Michael.Halassa@nyumc.org.

Author Contributions

MMH conceived, designed the project and collected data. MMH and ZC analyzed the electrophysiological and behavioral data. ZC developed novel computational methods for data analysis. RDW and PMB developed technical aspects of the attentional task. RDW collected data for the optogenetic tagging experiments. SZ and FW provided retrograde viruses. BZ developed and adapted quantitative structural connectivity methods and provided input on their inclusion in the manuscript. ENB provided input and oversight on statistical analysis. MAW supervised the study. MMH wrote the paper with input from MAW.

manipulation of these TRN sub-networks. Our findings provide evidence for differential regulation of thalamic inhibition across brain states, suggesting that the TRN separately controls external stimulus processing and internally-generated computations, a basic determinant of cognitive function.

Introduction

How does the brain switch between processing of information originating from different sources to successfully guide behavior? How does it flexibly shift between processing of external stimuli and internal constructs to optimize cognitive performance? Answers to these questions will not only enhance our understanding of the neural basis of cognition, but will likely refine our concepts of brain disorders in which cognitive dysfunction is central (Stefansson et al., 2014). In humans, the shift between external and internal goal-directed cognition is known to recruit distinct cortical networks (Buckner and Krienen, 2013). For example, the default mode network, which includes medial prefrontal cortex, is suppressed during tasks that demand external attention but activated when subjects perform internally-guided behaviors (Spreng et al., 2010). In contrast, the dorsal attentional network, which includes dorsolateral prefrontal cortex, is activated during external attention (Fox et al., 2005). Electrophysiological recordings in non-human primates have shown that interactions among circuits of the dorsal attentional network are achieved through synchronous oscillatory dynamics (Miller and Buschman, 2012). Prefrontal regions lead parietal regions in top-down attention, while parietal regions lead prefrontal ones in bottom-up attention (Buschman and Miller, 2007). While the circuit mechanisms underlying the establishment of these cortical oscillatory dynamic states are incompletely understood, recent experiments have shown that the thalamus may play a central role in cortico-cortical synchrony required for cognitive performance (Saalmann et al., 2012). These findings add to established knowledge on the role of thalamus in regulating cortical dynamics in sleep (Magnin et al., 2010; Steriade and Llinas, 1988), but raise important mechanistic questions on how the thalamus regulates cortical activity in an arousal state-dependent manner, a pre-requisite to understanding its precise role in cognitive function. Also, because the thalamus is functionally segregated into different nuclei (Jones, 2002), it may allow for establishing a multitude of cortical states depending on the type and number of nuclei engaged during a particular behavior.

Broad shifts in arousal offer an opportunity to study circuit mechanisms of how the brain switches between processing external stimuli and internally-generated activity. Several studies have delineated cortical mechanisms by which processing of sensory information is broadly suppressed during sleep (Issa and Wang, 2011; Livingstone and Hubel, 1981) but is enhanced in active waking (Livingstone and Hubel, 1981) and attentional states (Briggs et al., 2013; Desimone and Duncan, 1995), while others have established mechanisms by which offline limbic processing of memories is enhanced during sleep and quiet wakefulness (Buzsaki, 2010; Ji and Wilson, 2007; Karlsson and Frank, 2009). Within this framework, thalamo-cortical network engagement in processing of different information types is expected to occur in a state-dependent manner.

The thalamic reticular nucleus (TRN), a group of GABAergic neurons that provides inhibitory control over thalamic nuclei, is strategically positioned to selectively modulate thalamo-cortical network activation (Crick, 1984; Pinault, 2004). In fact, based on its anatomical connections, Francis Crick postulated that "if the thalamus is the gateway to the cortex, the reticular complex might be described as the guardian of the gateway" (Crick, 1984). The TRN has been implicated in sensory processing where its neurons exhibit complex visual receptive fields (Vaingankar et al., 2012) and respond to deviant (odd-ball) auditory stimuli (Yu et al., 2009). In behaving primates, visual TRN neurons are modulated by selective attention (McAlonan et al., 2008). The TRN has also been linked to internal processing during sleep, where its activity is associated with sleep rhythms and behavior (Cueni et al., 2008; Espinosa et al., 2008; Huguenard and McCormick, 2007), and its neurons are known to exhibit rhythmicity in relation to spindle oscillations (Steriade et al., 1986), 9-15Hz dynamics that are observed in the cortex during sleep, which correlate with sleep stability (Dang-Vu et al., 2010), and sleep-dependent memory consolidation (Diekelmann and Born, 2010; Eschenko et al., 2006). How the TRN operates to support these different state-dependent functions is unclear, in part, due to a gap in knowledge about how TRN microcircuits are functionally organized. Physiological attributes of thalamic nuclei are known to depend on their anatomical connections (Jones, 1981), but the TRN has traditionally been viewed as a monolithic structure, with no link between its connectivity and function. While recent work in primates has shown distinct connectivity patterns for sensory and limbic TRN (Zikopoulos and Barbas, 2012), the impact of these anatomical substrates on thalamo-cortical function has remained unknown given the lack of physiological studies.

We directly addressed this gap in knowledge by recording from TRN ensembles in naturally behaving mice. Our recordings revealed a previously unknown functional diversity within TRN microcircuits. Specifically, two functional sub-populations of TRN neurons were identified that exhibited opposite modulation by sleep and attentional states. Connectivity and genetic-based dissection of intact TRN microcircuits revealed an anatomical basis for this functional segregation. Specifically, sensory-projecting neurons exhibited activity patterns consistent with inhibition of sensory processing during sleep but its augmentation during attentional states, while limbic-connected neurons exhibited little activity during sleep, likely enhancing offline limbic processing. TRN-specific optogenetic manipulations revealed its causal role in attentional performance, an effect that was recapitulated by selective sensory TRN sub-network manipulation. Together, our data show that the TRN consists of connectivity-based functional sub-networks that differentially participate in sensory and limbic processing in a state-dependent manner. This architecture may facilitate switching of cortical information processing between externally-driven and internally-generated computations, a basic determinant of cognitive function.

Results

TRN recordings in the freely behaving preparation

To obtain stable recordings of TRN ensembles in mice during free behavior, we implanted arrays of adjustable extracellular recording electrodes targeting the dorsal pole of this brain

structure (Fig. 1A), which is known to be connected to both anterior limbic (Cornwall et al., 1990) and visual sensory thalamic nuclei (Kimura et al., 2012). Electrode position was confirmed by physiological signals obtained during adjustment (Fig. 1, A to D), and post-mortem histology (Fig. 1, E and F). TRN neurons were identified by their thin spike waveform compared to relay neurons as has been done in recent studies (Gardner et al., 2013; Halassa et al., 2011) (Fig. 1G) and is normally performed for extracellular inhibitory neuronal identification in cortical (Cardin et al., 2009) and hippocampal recordings (Royer et al., 2012). Consistent with previous studies, many TRN neurons showed a bursting spike firing pattern most noticeable during slow wave sleep (SWS, 128/195, Fig. S1A, B), and about half of these neurons exhibited a particular burst structure (accelerando-decelerando) observed in other species (Marlinski et al., 2012; Vaingankar et al., 2012) (Fig. S1, C and D).

TRN neurons exhibit heterogeneous firing in relation to sleep spindle oscillations

One of the major functions attributed to TRN neurons is their role in generating spindle oscillations (Bazhenov et al., 2000; Contreras et al., 1993; Halassa et al., 2011). We examined the correlation between individual TRN neuronal rate functions and cortical electroencephalographic (EEG) spindle power in natural SWS (Fig. 2A, Fig. S2, A and B). Consistent with previous findings in unanesthetized cats (Steriade et al., 1986), we found that many TRN neurons were positively correlated with spindle power (Fig. 2A, Fig. S2B). However, surprisingly, we found that others were negatively correlated with this measure (Fig. 2A, Fig. S2B). Analysis of the correlation between TRN neuronal firing rates and cortical spindle power revealed a bimodal distribution (Fig. 2B, $n = 7$ mice). Neurons that were positively correlated to spindle power increased their firing rate specifically during spindle events (Fig. 2, C to E; see Fig. S2C and D for spindle detection examples), with stronger spindle-phase locking values observed for these neurons than negatively correlated ones (Fig. 2, F to H; see Fig. S2, E to F for unbiased detection of phase-locking). Conversely, neurons that were negatively correlated to spindle power were also negatively correlated to delta power (Fig. S2G), and exhibited a robust elevation in firing rate with increased arousal (arousal correlated, Fig. 2I). Thus, in SWS, two functional TRN sub-populations are observed: one that is spindle correlated (SC) and another that is arousal correlated (AC). Equivalent numbers of these neurons were recorded from all animals with high recording yield and they exhibited no difference in overall firing rates or burst properties (Table S1).

Spindle-correlated TRN neurons exhibit state-dependent modulation consistent with regulation of sensory processing

Slow wave sleep is a state in which the cortical surface EEG is dominated by slow waves in the delta range (0.5-4Hz). These dynamics are associated with coordinated changes of excitability across cortical neurons (Steriade et al., 1993; Vyazovskiy et al., 2009), and are known to influence excitability in cortically-connected structures (Hahn et al., 2009). We found that TRN neurons were modulated by cortical delta, with both SC and AC neurons exhibiting the same degree of delta phase locking values (Fig. 3, A to D). However, while SC neurons showed preferred firing during delta wave troughs (corresponding to UP states, assessed by cortical multiunit activity), AC neurons showed a broad delta phase distribution

(Fig. 3, E and F). The narrow delta phase distribution of SC neurons suggested an enhanced probability of coordinated spiking across this population, which was confirmed by a SWS-dependent increase in their spike-time synchrony (a short-latency cross-correlation measure, see Methods), compared to AC neurons (Fig. 3, G to I, Fig. S3). Because sensory processing is known to be diminished in SWS, this analysis suggested a role for SC neurons in enhanced inhibitory gating of sensory thalamic output during SWS. Exploratory behavioral experiments found that SC neurons were more likely to reduce their activity in a visual detection task, specifically during the period of elevated attentional load (Kahn et al., 2012), compared to AC neurons (Fig. S4). Together, these findings suggested selective participation of SC neurons in sensory processing across arousal states.

Optogenetics-assisted circuit dissection of TRN neurons reveals connectivity based subnetwork architecture

Because dorsal TRN projects to both sensory and limbic thalamus (Fig. S5), we asked whether functional attributes of SC and AC neurons were related to patterns of connectivity with thalamic targets. To enable selective targeting of the TRN, we used mice that expressed Cre recombinase (Cre) under the vesicular GABA transporter (VGAT) promoter (Vong et al., 2011). VGAT-Cre animals enabled selective expression of transgenes in the TRN, but not nearby thalamic nuclei, which do not contain VGAT positive neurons. This was achieved by injecting adeno-associated viruses (AAV) containing double-floxed cassettes, stereotactically into the TRN (Fig. S5A-F). To enable targeting of TRN neurons that project to specific thalamic nuclei, we used lentiviruses. These viruses exhibited two important attributes that resulted in connectivity-specific TRN neuronal tagging. First, because they were pseudotyped with a chimeric envelope protein composed of the extracellular and transmembrane domains of rabies virus glycoprotein (RG) and the cytoplasmic domain of VSV-G (see methods), they were taken up by axonal terminals in the thalamic target of interest and retrogradely transported. Second, these viruses were engineered to harbor double-floxed cassettes, and therefore only resulted in the expression of transgenes in the TRN when injected in VGAT-cre mice (Fig. S5, H to O). Using this strategy, we engineered retrograde lentiviruses with double-floxed cassettes containing the light activated ion channel channelrhodopsin-2 (ChR2) (Boyden et al., 2005; Fenno et al., 2011), and injected them into either sensory visual or anterior limbic thalamus of VGAT-Cre mice (Fig. 4, A and B). We performed extracellular recordings from optogenetically identified TRN neurons in three visual- and two anterior-injected mice while animals performed a visual detection task and in post-task sleep (Fig. 4, C and E). We identified visual thalamic-projecting or anterior complex-projecting neurons by their short-latency response to 10ms pulses of blue laser (5-10ms onset, Fig. 4, D and F). Visual-projecting neurons also showed a 30-50ms latency response to visual stimulation (Fig. 4, D and F). Electrode positions were additionally confirmed by postmortem histology (Fig. 4, G and H).

We found that visual-projecting TRN neurons were functionally different from limbic-projecting ones. Specifically, visual-connected neurons were mostly spindle-correlated (SC) (Fig. 5A), while limbic-projecting neurons were arousal correlated (AC) (Fig. 5, B and C). Visual-projecting neurons exhibited significantly higher phase-locking to spindles than limbic-projecting neurons (Fig. 5D). Consistent with a role for visual-projecting TRN in

state-dependent control of visual processing, these neurons exhibited elevated pairwise spike-time synchrony in SWS while limbic-projecting neurons did not (Fig. 5E).

To investigate the participation of these sub-networks in information processing beyond sleep, we trained mice on a visual detection task that required attentional engagement. The task required the animal to correctly detect a visual stimulus (500msec) and subsequently move towards it, obtaining food from a reward site positioned underneath the stimulus location. A white noise auditory stimulus signaled the ability to initiate a trial. A trial was successfully initiated when the mouse broke an infra-red beam continuously for 500-700ms, ensuring proper head orientation during visual stimulus presentation. To minimize impulsive poking, rewards were only made available for a period of fifteen seconds following successful initiation (Fig. 5F). The absence of a correlation between initiation time and latency to collect reward as well as elevated latency during catch trials confirmed timely and specific response to visual stimulus presentation (Fig. S6, A to C). We found a robust and specific reduction in firing rate for visual projecting TRN neurons following trial initiation, but no significant modulation of limbic projecting TRN neurons during the task (Fig. 5G). This result is consistent with the engagement of visual TRN sub-network in state-dependent sensory visual processing. Furthermore, because the modulation occurred in the period prior to stimulus presentation, it suggested the participation of these neurons in attentional states, where visual thalamic inhibition may be transiently reduced to augment subsequent sensory processing.

Temporally-precise TRN activation diminishes performance on the visual detection task

To investigate whether the observed TRN neuronal firing rate changes were causal for visual detection task performance, we employed optogenetic manipulations. First, we injected a cre-dependent AAV (serotype2) expressing channelrhodopsin into the TRN of VGAT-Cre mice, which resulted in selective TRN expression (Fig. 6A). Because visual TRN neurons exhibited reduction in firing rate between task initiation and stimulus presentation, we used optogenetic activation to offset this reduction. Our investigations showed that pulse trains of >40Hz (4-5 mW, 200μm fiber [140-180 $mW.mm^{-2}$]) results in sustained elevation of TRN neuronal firing rates and a concomitant reduction in their thalamic targets (Fig. 6B). We therefore used pulse trains of 50Hz frequency, pulse-width 2ms (duty cycle: 10%) to achieve a broad elevation of TRN firing rates throughout the initiation as well as stimulus presentation period (task stimulation). We found that this optogenetic stimulation regime resulted in a robust prolongation of latencies to collect reward in all mice examined (Fig. 6, C and E, Fig. S6, D and E, movie S1). This suggested that enhancing TRN neuronal firing rate during the window of elevated attentional demands was detrimental to behavior, supporting the notion that a sharp drop in a subset of TRN neuronal firing rates was important for optimal performance. To test whether the optogenetic effect was a result of diminished stimulus perception, we delivered a laser stimulation train of similar length that started upon stimulus presentation but avoided the initiation period (Fig. 6B). We found that this control stimulation did not impact performance on the task. Further, in support of the specificity of the optogenetic effect to the initiation period, we found that pulse trains of only 500ms limited to the post-initiation window resulted in diminished task performance (Fig. S6, D and E). Also consistent with the notion that TRN stimulation did not interfere

with stimulus perception, we found that this stimulation did not change the overall error rates in the task (Fig. S6D-E).

Temporally-precise TRN inhibition enhances attentional performance

The negative impact of TRN stimulation on task performance was consistent with the requirement for a subset of its neurons to reduce their firing rate during the attentional window. To fully test the causality of these physiological observations in the context of the task, we used eNpHR3.0 (Deisseroth and Schnitzer; Tye et al., 2011), a light-activated Cl^- pump that is known to hyperpolarize neurons and inhibit spiking, to determine whether further reducing TRN firing rate would improve performance. To increase the likelihood of observing a behavioral modulation, we subjected mice to mild sleep deprivation (1-3 hours, at the beginning of their rest phase) which resulted in slightly diminished task performance evident by prolonged latencies ($P < 0.05$, rank-sum test). Consistent with a causal role for TRN neurons in optimal task performance, we found that optogenetic inhibition of these neurons resulted in improved performance in all mice examined (Fig. 6, F to H, Fig. S6, F and G, movie S2).

To test whether these effects were sub-network specific we performed bi-directional optogenetic manipulations in retrogradely-labelled TRN neuronal populations during the task (Fig. 6I). We retrogradely labeled visual-connected and limbic-connected TRN neurons with either ChR2 or eNpHR3.0. We found that ChR2-mediated activation of the visual-projecting TRN during the attentional window of the visual detection task diminished performance, while its inhibition augmented performance. In contrast, neither activation nor inhibition of limbic-projecting TRN impacted performance (Fig. 6J), consistent with the observation that these neurons are not significantly modulated during that phase of the task (Fig. 5). These data also suggest that earlier results obtained with bi-directional manipulations of the TRN may be fully explained by effects on sensory-projecting neurons, a population that overlaps with the SC neurons identified earlier in this study. Our findings are unlikely to be explained by differences in optogenetic targeting, as comparable proportions of TRN neurons were tagged in these two preparations (anterior-projecting: 31/100; visual-projecting: 52/190). In addition, there was no impact on error rates for any of these manipulations. Because the observed effects could be explained by neither sensory nor motor deficits, we suggest that they are likely cognitive. Also, because they occurred during the stimulus expectation period of the task, they are consistent with the involvement of TRN neurons in attentional states.

Discussion

A major attribute of cognitive function is the ability to flexibly switch between processing different types of information. Broad shifts in arousal states offer an opportunity to examine how the brain switches from external stimulus processing in wake to internal memory processing in sleep. By regulating the interactions within thalamo-cortical networks, the thalamic reticular nucleus (TRN) has been hypothesized to play an important role in cognitive function (Zikopoulos and Barbas, 2012). However, the precise nature of this regulation has been difficult to discern given the relative inaccessibility of TRN to

physiological recordings. As such, and in the absence of concrete experimental data, the TRN has traditionally been viewed as a monolithic structure, providing uniform inhibition to thalamic nuclei (Crick, 1984; Llinas and Steriade, 2006). In such a regime, it is unclear how the brain would be able to selectively control the interactions between functionally segregated thalamic nuclei and their cortical targets.

In this study, we have systematically examined the functional architecture of the thalamic reticular nucleus in the freely behaving mouse. We found that the TRN is composed of functionally segregated sub-networks defined by anatomical connectivity. Sensory-projecting TRN regulates sensory processing in a state-dependent manner, while limbic-projecting TRN exhibits little activity during quiescent states, perhaps enabling the engagement of its thalamic target in offline processing associated with other limbic circuits (e.g. hippocampal reactivation). Additionally, inhibiting sensory-projecting TRN neurons during attentional states results in enhanced performance on a visual discrimination task, identifying this sub-network as a possible target for cognitive enhancement (evident by reduced latency for sensory detection). Overall, our data show that the functional architecture of TRN sub-networks may have essential roles in mediating the impact of arousal states on higher level cognitive function (Koch, 1993), and that it may be utilized in state-dependent switching between sensory transmission and offline processing (Fig. 7).

Functionally distinct TRN sub-networks

Our initial recordings were in the dorso-rostral part of the mouse TRN (Fig. 1), where reticular neurons are known to project to anterior (Cornwall et al., 1990) as well as visual sensory nuclei (Kimura et al., 2012) (Fig. S5). In agreement with previous recordings in cats (Steriade et al., 1986), we found that many TRN neurons increased their firing rate with elevation in cortical spindle power. Our subsequent finding that visual sensory TRN neurons are likely to exhibit this attribute as well as phase-lock to spindles is consistent with recordings from the somatosensory TRN in freely behaving rats (Marks and Roffwarg, 1993). The finding of a separate sub-population of TRN neurons (arousal correlated) is unexpected, and its link to limbic processing might have been previously missed because earlier studies did not target limbic-projecting sectors of the TRN. In contrast to sensory-projecting TRN neurons, these neurons exhibited broad modulation by arousal state as seen in cortical (Vyazovskiy et al., 2009) and thalamo-cortical neurons (Weyand et al., 2001). Functional divergence of sensory and limbic TRN subnetworks was further evident during behavior in the visual detection task, where sensory neurons showed a sharp reduction in firing rate following task initiation (Fig. 5), while limbic neurons did not. Interestingly, limbic projecting neurons had comparable firing rates to AC neurons recorded in the first data set (Table S2 vs. Table S1). However, visual projecting neurons had different firing rates than SC neurons recorded earlier in the study. This may have been related to visual-projecting neurons being recorded from more caudal parts of the TRN (Fig. 1 vs. Fig. 4).

The impact of TRN on cognitive function

The reduction in firing rate observed for sensory TRN neurons during the task window in which attentional demands were highest suggests the engagement of these neurons in attentional state modulation. It is important to note that this modulation is probably distinct

from the role of TRN in selective attention shown by studies in primates (McAlonan et al., 2008), which have revealed a correlation between neural responses and task accuracy, rather than speed. Our task has examined TRN involvement in the behavioral state preceding stimulus detection. Because mice perform this task with high accuracy, their variability in performance is seen mostly in latency, which is likely to reflect variability in attentional state (a form of arousal), rather than selective attention. Our physiological results as well as optogenetic manipulations corroborate this notion, demonstrating that a reduction in sensory TRN firing rates is required for optimal task performance. Because neither a sensory or motor effect was observed in these studies, we interpret these findings to reveal a permissive cognitive role for TRN in attentional states. This interpretation is consistent with the role of state-dependent cortical dynamics in accumulation of evidence required for decision-making (Brunton et al., 2013; Kubanek et al., 2013).

The involvement of TRN in cognitive function offers a unique perspective on connecting a number of concepts in neuroscience that had previously been studied separately. For example, while our study examined the participation of TRN microcircuits in sleep and attentional states separately, the sub-network architecture of TRN may allow for flexible switching between processing of external input and internal constructs in cognitive tasks, facilitating selective thalamo-cortical network engagement (Roth et al., 2009). Interestingly, recent experiments in humans have shown that rapid changes in arousal measures, such as pupil diameter, predict successful performance on cognitive tasks requiring the use of external information to update internal beliefs (Nassar et al., 2012). Given the state-dependent modulation of TRN neurons, these microcircuits may offer a mechanistic link between subtle changes in arousal and cognitive performance. In addition, these sub-networks offer a mammalian example of how the same neurons can switch their functionality in a behaviorally-relevant manner, a long recognized attribute of small circuits in model systems (Bargmann and Marder, 2013).

Our findings also offer a unique perspective on cognitive dysfunction, which appears to be central to a number of neurodevelopmental and neuropsychiatric disorders (Coe et al., 2012; Stefansson et al., 2014). While inhibitory circuits have long been recognized to be disrupted in several of these disorders, the focus has been on cortical interneurons (Gonzalez-Burgos and Lewis, 2012). Dissecting TRN microcircuit architecture and examining its participation in cognitive function is a first step in understanding how its dysfunction may contribute to brain disorders. Given the role of thalamus in regulating cortical states, it would not be surprising that its inhibitory dysfunction contributes to a number of brain disorders (Barch and Ceaser, 2012; Fitzgerald et al., 2000).

Spindle-related microcircuitry

Our findings that TRN neurons associated with spindle oscillations influence thalamic sensory processing in a state-dependent fashion provide a mechanism for the link between spindles and sleep stability (Dang-Vu et al., 2010; Wimmer et al., 2012). In addition, they link sensory processing in sleep to that during attentional states, which to our knowledge, has never been explicitly demonstrated. Spindle-associated TRN microcircuits, controlling sensory processing across states of vigilance may explain the long recognized association

between spindles and cognitive performance (Fogel and Smith, 2010), and may relate to the association between spindles and cognitive dysfunction in schizophrenia (Ferrarelli et al., 2010; Keshavan et al., 2011).

Relevance to offline processing

Could our findings be placed in a larger context of hippocampal-thalamo-cortical interaction underlying online behavior versus offline memory processing? We think yes. The hippocampus sends monosynaptic input to cingulate and retrosplenial cortices, areas that are connected to the anterior thalamic complex. Damage to any of these structures is known to result in spatial memory deficits (Rolls, 2013). As such, limbic TRN activity may be permissive to offline hippocampal-thalamo-cortical interactions evident by reduced firing rate of these neurons during SWS (Fig. 5). The elevated firing of these neurons during active wakefulness may set a higher inhibitory tone in the anterior complex during behavioral arousal. The role of this inhibition in shaping online processing of these neurons, and their engagement in behavior is an open but intriguing question.

The role of hippocampus and associated limbic circuitry in memory processing extends well beyond sleep, as hippocampal-cortical interactions are required for basic cognitive tasks requiring online encoding and retrieval of memories (Preston and Eichenbaum, 2013). Recent findings of default-mode network engagement in these tasks suggest large network functional organization (Ward et al., 2013), in which thalamic modulation of cortical dynamics may be necessary. The role of TRN in these large scale functional interactions will undoubtedly be an exciting area of investigation, with broad basic and translational implications.

Experimental Procedures

Animals

Seven 4-6 month old male mice in a C57Bl6/J background were used for the first data set (Figs. 1-3). Three VGAT-Cre mice were used for visual thalamic optogenetic tagging and two mice used for anterior thalamic optogenetic tagging (Figs. 4 and 5). Four VGAT-Cre mice were used for the optogenetic activation experiments and four others were used for the optogenetic inhibition (Fig. 6). A total of seven VGAT-Cre mice were used for histology experiments (Fig. S1). All research involving mice have been conducted according to the Institutional Animal Care and Use Committee (IACUC) guidelines at MIT. All procedures were approved by the IACUC.

Electrophysiological recording

Following recovery, each animal was connected to two 16-channel preamplifier headstages or a single, custom made 32-channel preamplifier headstage (Neuralynx, Bozeman, MT). All data were recorded using a Neuralynx Digilynx recording system. Signals from each stereotrode were amplified, filtered between 0.1 Hz and 9 kHz and digitized at approximately 30 kHz. Local field potentials (LFPs) were collected from a single channel on each stereotrode. The LFP and EEG traces were amplified and filtered between 0.1 Hz and 30 kHz. The EEG was acquired as a referential signal between the ipsilateral frontal lead (at

approximately A/P: +0.5mm, M/L: 0.5mm, D/V, 0.1-0.2mm, directed at cingulate) and cerebellar reference. For experiments involving the tagging of visual neurons, the EEG was a referential signal between primary visual cortex and the cerebellum. Stereotrodes were slowly lowered (over several days) in 125-250 micron steps. Spike sorting was performed offline using the MClust toolbox (http://redishlab.neuroscience.umn.edu/mclust/MClust.html), based on spike amplitudes and energies on the two electrodes of each stereotrode. Units were separated by hand, and cross-correlation and autocorrelation analyses were used to confirm unit separation.

Virus injections

For anatomical tracing experiments, AAV-hSyn-DIO-EGFP (serotype 2) was injected at multiple volumes (200nL – 1μL) into thalamus of VGAT-Cre animals (A/P, −0.6mm to −1.0mm, M/L: 0.9mm; D/V −3.5mm) unilaterally. Animals were allowed to recover for at least 3 weeks for optimal virus expression, after which they were prepared for histological experiments.

For optogenetic manipulation experiments, AAV-EF1α-DIO-ChR2-EYFP and AAV-EF1α-DIO-eNpHR3.0-EYFP (all serotype 2) were used. These viruses were produced by the vector core at UNC Chapel Hill with titers around 10^{12} VG/mL. Viruses (250-350nl) were injected bilaterally into TRN of VGAT-cre mice (A/P, −0.6mm; ±M/L: 0.9mm; D/V −3.5mm) using a quintessential stereotactic injector (Stoelting, #53311). Mice were allowed to recover for 2-4 weeks following injection to allow for virus expression. For retrograde histological tracing and optogenetic tagging experiments (Figs. 5 and S5), pseudotyped retrograde lentiviruses (RG-LV) were used. Visually connected TRN neurons were labelled through virus injections (0.5-0.8μl) into visual thalamus (AP, −2.1mm, ML, 2mm, DV, 2.5mm) whereas anterior thalamic connected TRN neurons were targeted through injections into the anterior complex (AP, −0.7mm, ML, 0.65mm, DV, −2.6mm). RG-LV contained the EF1α promoter, followed by a double flox cassette in which the floxed gene (in reverse orientation) was either EGFP, channelrhodopsin (ChR2), or halorhodopsin (eNpHR3.0), and followed by the woodchuck posttranscriptional regulatory element (WPRE). All vectors were modified from the original lentivector pFCGW. For production of the viral vector, the expression plasmid along with two helper plasmids Δ8.9 and FuG–B2 (a chimeric envelope protein composed of the extracellular and transmembrane domains of rabies virus glycoprotein (RG) and the cytoplasmic domain of VSV-G; pCAGGS–FuG– B2; a gift from Kazuto Kobayashi, Fukushima Medical University, Fukushima, Japan), were transfected into HEK293T cells with Lipofectamine2000 (Invitrogen). Viral particles were collected from the cell culture medium, pelleted by ultracentrifugation at 65,000 ×g (m/s2) for 2.5 h, resuspended in PBS, washed and concentrated using Amicon Ultra 4. Titers were between 10^8-10^9 VG/mL. Mice were allowed 4-6 weeks of recovery following surgery to allow for retrograde virus expression.

On-line optogenetic tagging of TRN units

A fiber optic patch cord (Doric Lenses) delivered light from a 473 nm laser (Opto Engine, Midvale, UT) to the fiber optic connector on the animal's implant. Prior to connecting to the animal, laser power was measured and titrated to ~10 mW using a neutral density filter

(Thorlabs, Newton, NJ). Power at the tip of the implanted fiber was ~50% of this value, based on measurements prior to surgery. Thus, there was 4-5 mW of power at the fiber tip, or 140-180 $mW.mm^{-2}$ for a 200-μm fiber. An analog stimulus generator was used to control laser pulses of 10 ms duration and 0.01 Hz frequency.

Supplementary Material

Refer to Web version on PubMed Central for supplementary material.

Acknowledgments

We thank L. Acsady for helpful comments as well as all members of the Wilson laboratory. M.M.H. is supported by an NIH pathway to independence career award (K99 NS 078115) from the NINDS and a NARSAD Young Investigator Award. Z.C. is supported by an NSF-CRCNS grant (award IIS-1307645) and an Early Career Award (Mathematical Biosciences Institute). BZ is supported by grants from NIMH (R01MH101209, R01MH057414) and NSF (CELEST, SBE-0354378). F.W. is supported by NIH grants (R01NS077986, DP1MH103908). E.N.B and M.A.W are supported by a transformative R01 award (TR01-GM10498). M.A.W. is additionally supported by NIH grant R01-MH061976.

References

Barch DM, Ceaser A. Cognition in schizophrenia: core psychological and neural mechanisms. Trends Cogn Sci. 2012; 16:27–34. [PubMed: 22169777]

Bargmann CI, Marder E. From the connectome to brain function. Nat Methods. 2013; 10:483–490. [PubMed: 23866325]

Bazhenov M, Timofeev I, Steriade M, Sejnowski T. Spiking-bursting activity in the thalamic reticular nucleus initiates sequences of spindle oscillations in thalamic networks. J Neurophysiol. 2000; 84:1076–1087. [PubMed: 10938329]

Boyden ES, Zhang F, Bamberg E, Nagel G, Deisseroth K. Millisecond-timescale, genetically targeted optical control of neural activity. Nat Neurosci. 2005; 8:1263–1268. [PubMed: 16116447]

Briggs F, Mangun GR, Usrey WM. Attention enhances synaptic efficacy and the signal-to-noise ratio in neural circuits. Nature. 2013; 499:476–480. [PubMed: 23803766]

Brunton BW, Botvinick MM, Brody CD. Rats and humans can optimally accumulate evidence for decision-making. Science. 2013; 340:95–98. [PubMed: 23559254]

Buckner RL, Krienen FM. The evolution of distributed association networks in the human brain. Trends Cogn Sci. 2013; 17:648–665. [PubMed: 24210963]

Buschman TJ, Miller EK. Top-down versus bottom-up control of attention in the prefrontal and posterior parietal cortices. Science. 2007; 315:1860–1862. [PubMed: 17395832]

Buzsaki G. Neural syntax: cell assemblies, synapsembles, and readers. Neuron. 2010; 68:362–385. [PubMed: 21040841]

Cardin JA, Carlen M, Meletis K, Knoblich U, Zhang F, Deisseroth K, Tsai LH, Moore CI. Driving fast-spiking cells induces gamma rhythm and controls sensory responses. Nature. 2009; 459:663–667. [PubMed: 19396156]

Coe BP, Girirajan S, Eichler EE. The genetic variability and commonality of neurodevelopmental disease. Am J Med Genet C Semin Med Genet. 2012; 160C:118–129. [PubMed: 22499536]

Contreras D, Curro Dossi R, Steriade M. Electrophysiological properties of cat reticular thalamic neurones in vivo. J Physiol. 1993; 470:273–294. [PubMed: 8308730]

Cornwall J, Cooper JD, Phillipson OT. Projections to the rostral reticular thalamic nucleus in the rat. Exp Brain Res. 1990; 80:157–171. [PubMed: 2358025]

Crick F. Function of the thalamic reticular complex: the searchlight hypothesis. Proc Natl Acad Sci U S A. 1984; 81:4586–4590. [PubMed: 6589612]

Cueni L, Canepari M, Lujan R, Emmenegger Y, Watanabe M, Bond CT, Franken P, Adelman JP, Luthi A. T-type Ca2+ channels, SK2 channels and SERCAs gate sleep-related oscillations in thalamic dendrites. Nat Neurosci. 2008; 11:683–692. [PubMed: 18488023]

Dang-Vu TT, McKinney SM, Buxton OM, Solet JM, Ellenbogen JM. Spontaneous brain rhythms predict sleep stability in the face of noise. Curr Biol. 2010; 20:R626–627. [PubMed: 20692606]

Deisseroth K, Schnitzer MJ. Engineering approaches to illuminating brain structure and dynamics. Neuron. 80:568–577. [PubMed: 24183010]

Desimone R, Duncan J. Neural mechanisms of selective visual attention. Annu Rev Neurosci. 1995; 18:193–222. [PubMed: 7605061]

Diekelmann S, Born J. The memory function of sleep. Nat Rev Neurosci. 2010; 11:114–126. [PubMed: 20046194]

Eschenko O, Molle M, Born J, Sara SJ. Elevated sleep spindle density after learning or after retrieval in rats. J Neurosci. 2006; 26:12914–12920. [PubMed: 17167082]

Espinosa F, Torres-Vega MA, Marks GA, Joho RH. Ablation of Kv3.1 and Kv3.3 potassium channels disrupts thalamocortical oscillations in vitro and in vivo. J Neurosci. 2008; 28:5570–5581. [PubMed: 18495891]

Fenno L, Yizhar O, Deisseroth K. The development and application of optogenetics. Annu Rev Neurosci. 2011; 34:389–412. [PubMed: 21692661]

Ferrarelli F, Peterson MJ, Sarasso S, Riedner BA, Murphy MJ, Benca RM, Bria P, Kalin NH, Tononi G. Thalamic Dysfunction in Schizophrenia Suggested by Whole-Night Deficits in Slow and Fast Spindles. Am J Psychiatry. 2010; 167:1339–1348. [PubMed: 20843876]

Fitzgerald KD, Moore GJ, Paulson LA, Stewart CM, Rosenberg DR. Proton spectroscopic imaging of the thalamus in treatment-naive pediatric obsessive-compulsive disorder. Biol Psychiatry. 2000; 47:174–182. [PubMed: 10682215]

Fogel SM, Smith CT. The function of the sleep spindle: a physiological index of intelligence and a mechanism for sleep-dependent memory consolidation. Neurosci Biobehav Rev. 2010; 35:1154–1165. [PubMed: 21167865]

Fox MD, Snyder AZ, Vincent JL, Corbetta M, Van Essen DC, Raichle ME. The human brain is intrinsically organized into dynamic, anticorrelated functional networks. Proc Natl Acad Sci U S A. 2005; 102:9673–9678. [PubMed: 15976020]

Gardner RJ, Hughes SW, Jones MW. Differential spike timing and phase dynamics of reticular thalamic and prefrontal cortical neuronal populations during sleep spindles. J Neurosci. 2013; 33:18469–18480. [PubMed: 24259570]

Gonzalez-Burgos G, Lewis DA. NMDA Receptor Hypofunction, Parvalbumin-Positive Neurons and Cortical Gamma Oscillations in Schizophrenia. Schizophr Bull. 2012

Hahn TT, McFarland JM, Berberich S, Sakmann B, Mehta MR. Spontaneous persistent activity in entorhinal cortex modulates cortico-hippocampal interaction in vivo. Nat Neurosci. 2009; 15:1531–1538. [PubMed: 23042081]

Halassa MM, Siegle JH, Ritt JT, Ting JT, Feng G, Moore CI. Selective optical drive of thalamic reticular nucleus generates thalamic bursts and cortical spindles. Nat Neurosci. 2011; 14:1118–1120. [PubMed: 21785436]

Huguenard JR, McCormick DA. Thalamic synchrony and dynamic regulation of global forebrain oscillations. Trends Neurosci. 2007; 30:350–356. [PubMed: 17544519]

Issa EB, Wang X. Altered neural responses to sounds in primate primary auditory cortex during slow-wave sleep. J Neurosci. 2011; 31:2965–2973. [PubMed: 21414918]

Ji D, Wilson MA. Coordinated memory replay in the visual cortex and hippocampus during sleep. Nat Neurosci. 2007; 10:100–107. [PubMed: 17173043]

Jones EG. Functional subdivision and synaptic organization of the mammalian thalamus. Int Rev Physiol. 1981; 25:173–245. [PubMed: 6110641]

Jones EG. Thalamic organization and function after Cajal. Prog Brain Res. 2002; 136:333–357. [PubMed: 12143393]

Kahn JB, Ward RD, Kahn LW, Rudy NM, Kandel ER, Balsam PD, Simpson EH. Medial prefrontal lesions in mice impair sustained attention but spare maintenance of information in working memory. Learn Mem. 2012; 19:513–517. [PubMed: 23073640]

Karlsson MP, Frank LM. Awake replay of remote experiences in the hippocampus. Nat Neurosci. 2009; 12:913–918. [PubMed: 19525943]

Keshavan MS, Montrose DM, Miewald JM, Jindal RD. Sleep correlates of cognition in early course psychotic disorders. Schizophr Res. 2011; 131:231–234. [PubMed: 21724373]

Kimura A, Yokoi I, Imbe H, Donishi T, Kaneoke Y. Distinctions in burst spiking between thalamic reticular nucleus cells projecting to the dorsal lateral geniculate and lateral posterior nuclei in the anesthetized rat. Neuroscience. 2012; 226:208–226. [PubMed: 22989916]

Koch C. Computational approaches to cognition: the bottom-up view. Curr Opin Neurobiol. 1993; 3:203–208. [PubMed: 8513233]

Kubanek J, Snyder LH, Brunton BW, Brody CD, Schalk G. A low-frequency oscillatory neural signal in humans encodes a developing decision variable. Neuroimage. 2013; 83:795–808. [PubMed: 23872495]

Livingstone MS, Hubel DH. Effects of sleep and arousal on the processing of visual information in the cat. Nature. 1981; 291:554–561. [PubMed: 6165893]

Llinas RR, Steriade M. Bursting of thalamic neurons and states of vigilance. J Neurophysiol. 2006; 95:3297–3308. [PubMed: 16554502]

Magnin M, Rey M, Bastuji H, Guillemant P, Mauguiere F, Garcia-Larrea L. Thalamic deactivation at sleep onset precedes that of the cerebral cortex in humans. Proc Natl Acad Sci U S A. 2010; 107:3829–3833. [PubMed: 20142493]

Marks GA, Roffwarg HP. Spontaneous activity in the thalamic reticular nucleus during the sleep/wake cycle of the freely-moving rat. Brain Res. 1993; 623:241–248. [PubMed: 8221106]

Marlinski V, Sirota MG, Beloozerova IN. Differential gating of thalamocortical signals by reticular nucleus of thalamus during locomotion. J Neurosci. 2012; 32:15823–15836. [PubMed: 23136421]

McAlonan K, Cavanaugh J, Wurtz RH. Guarding the gateway to cortex with attention in visual thalamus. Nature. 2008; 456:391–394. [PubMed: 18849967]

Miller EK, Buschman TJ. Cortical circuits for the control of attention. Curr Opin Neurobiol. 2012; 23:216–222. [PubMed: 23265963]

Nassar MR, Rumsey KM, Wilson RC, Parikh K, Heasly B, Gold JI. Rational regulation of learning dynamics by pupil-linked arousal systems. Nat Neurosci. 2012; 15:1040–1046. [PubMed: 22660479]

Pinault D. The thalamic reticular nucleus: structure, function and concept. Brain Res Brain Res Rev. 2004; 46:1–31. [PubMed: 15297152]

Preston AR, Eichenbaum H. Interplay of hippocampus and prefrontal cortex in memory. Curr Biol. 2013; 23:R764–773. [PubMed: 24028960]

Rolls ET. Limbic systems for emotion and for memory, but no single limbic system. Cortex. 2013

Roth JK, Johnson MK, Raye CL, Constable RT. Similar and dissociable mechanisms for attention to internal versus external information. Neuroimage. 2009; 48:601–608. [PubMed: 19595772]

Royer S, Zemelman BV, Losonczy A, Kim J, Chance F, Magee JC, Buzsaki G. Control of timing, rate and bursts of hippocampal place cells by dendritic and somatic inhibition. Nat Neurosci. 2012; 15:769–775. [PubMed: 22446878]

Saalmann YB, Pinsk MA, Wang L, Li X, Kastner S. The pulvinar regulates information transmission between cortical areas based on attention demands. Science. 2012; 337:753–756. [PubMed: 22879517]

Spreng RN, Stevens WD, Chamberlain JP, Gilmore AW, Schacter DL. Default network activity, coupled with the frontoparietal control network, supports goal-directed cognition. Neuroimage. 2010; 53:303–317. [PubMed: 20600998]

Stefansson H, Meyer-Lindenberg A, Steinberg S, Magnusdottir B, Morgen K, Arnarsdottir S, Bjornsdottir G, Walters GB, Jonsdottir GA, Doyle OM, et al. CNVs conferring risk of autism or schizophrenia affect cognition in controls. Nature. 2014; 505:361–366. [PubMed: 24352232]

Steriade M, Domich L, Oakson G. Reticularis thalami neurons revisited: activity changes during shifts in states of vigilance. J Neurosci. 1986; 6:68–81. [PubMed: 3944624]

Steriade M, Llinas RR. The functional states of the thalamus and the associated neuronal interplay. Physiol Rev. 1988; 68:649–742. [PubMed: 2839857]

Steriade M, Nunez A, Amzica F. A novel slow (< 1 Hz) oscillation of neocortical neurons in vivo: depolarizing and hyperpolarizing components. J Neurosci. 1993; 13:3252–3265. [PubMed: 8340806]

Tye KM, Prakash R, Kim SY, Fenno LE, Grosenick L, Zarabi H, Thompson KR, Gradinaru V, Ramakrishnan C, Deisseroth K. Amygdala circuitry mediating reversible and bidirectional control of anxiety. Nature. 2011; 471:358–362. [PubMed: 21389985]

Vaingankar V, Sanchez Soto C, Wang X, Sommer FT, Hirsch JA. Neurons in the thalamic reticular nucleus are selective for diverse and complex visual features. Front Integr Neurosci. 2012; 6:118. [PubMed: 23269915]

Vong L, Ye C, Yang Z, Choi B, Chua S Jr. Lowell BB. Leptin action on GABAergic neurons prevents obesity and reduces inhibitory tone to POMC neurons. Neuron. 2011; 71:142–154. [PubMed: 21745644]

Vyazovskiy VV, Olcese U, Lazimy YM, Faraguna U, Esser SK, Williams JC, Cirelli C, Tononi G. Cortical firing and sleep homeostasis. Neuron. 2009; 63:865–878. [PubMed: 19778514]

Ward AM, Schultz AP, Huijbers W, Van Dijk KR, Hedden T, Sperling RA. The parahippocampal gyrus links the default-mode cortical network with the medial temporal lobe memory system. Hum Brain Mapp. 2013; 35:1061–1073. [PubMed: 23404748]

Weyand TG, Boudreaux M, Guido W. Burst and tonic response modes in thalamic neurons during sleep and wakefulness. J Neurophysiol. 2001; 85:1107–1118. [PubMed: 11247981]

Wimmer RD, Astori S, Bond CT, Rovo Z, Chatton JY, Adelman JP, Franken P, Luthi A. Sustaining sleep spindles through enhanced SK2-channel activity consolidates sleep and elevates arousal threshold. J Neurosci. 2012; 32:13917–13928. [PubMed: 23035101]

Yu XJ, Xu XX, He S, He J. Change detection by thalamic reticular neurons. Nat Neurosci. 2009; 12:1165–1170. [PubMed: 19684591]

Zikopoulos B, Barbas H. Pathways for emotions and attention converge on the thalamic reticular nucleus in primates. J Neurosci. 2012; 32:5338–5350. [PubMed: 22496579]

Highlights

- Connectivity-based optogenetic TRN dissection reveals a sub-network architecture
- Sensory-projecting TRN regulates cortical processing across sleep and attention
- Limbic-projecting TRN shows general regulation by arousal
- Optogenetic suppression of visual-projecting TRN in attention enhances performance

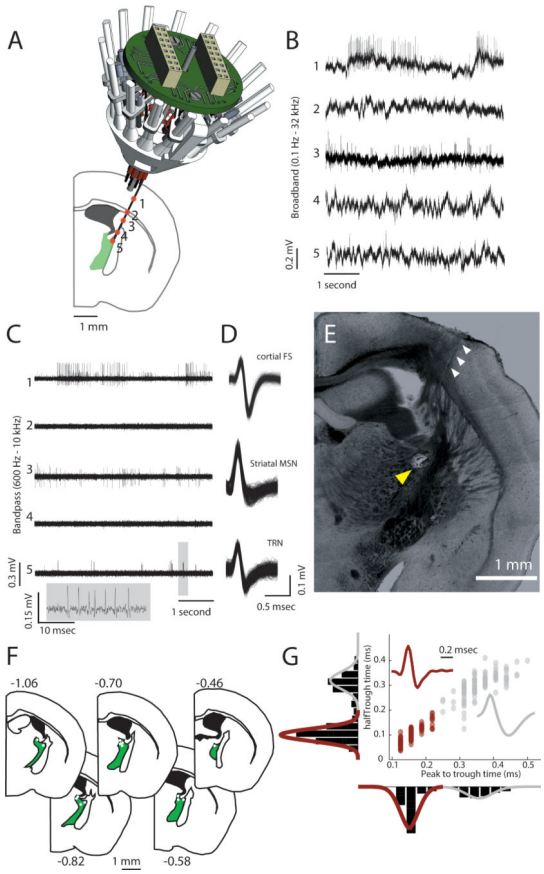

Figure 1. Independently adjustable multi-electrode recordings in the TRN

(A) The dorsal part of TRN was targeted by implanting an independently adjustable multi-electrode implant (16 independently movable microdrives, only 6-12 loaded in any experiment) at 15-degree angle relative to midline. Numbers denote different anatomical structures at which physiological recordings were made and shown in **B** and **C. (B)** Broadband (0.1Hz-32kHz) signal recorded at the different anatomical stations show the physiological trajectory of the recordings. Note the absence of spiking in the two white matter crossings (corpus callosum, 2 and internal capsule, 4). **(C)** Bandpass filtered signal (600Hz-10kHz) of traces in **B** showing spike trains. **(D)** Clustered neurons from traces 1, 3 and 5 showing the waveforms of a putative cortical fast spiking interneuron (top), a striatal medium spiny neuron (middle) and finally a TRN neuron (bottom), highlighted inset shows a burst event of this unit, exhibiting the accelerando-decelerando burst structure previously described. **(E)** Histological verification of the recording by electrode track (white arrowheads) and lesion at the tip (yellow arrowheads). **(F)** Distribution of TRN lesions seen across 6 out of 7 mice recorded. Numbers denote A/P distance from Bregma in mm. **(G)** A total of 195 putative TRN units with “thin” spikes were recorded (crimson), which had significantly different spike waveform features (peak-to-trough time and trough halfwidth) than 102 putative thalamic units (red). See also Fig. S1.

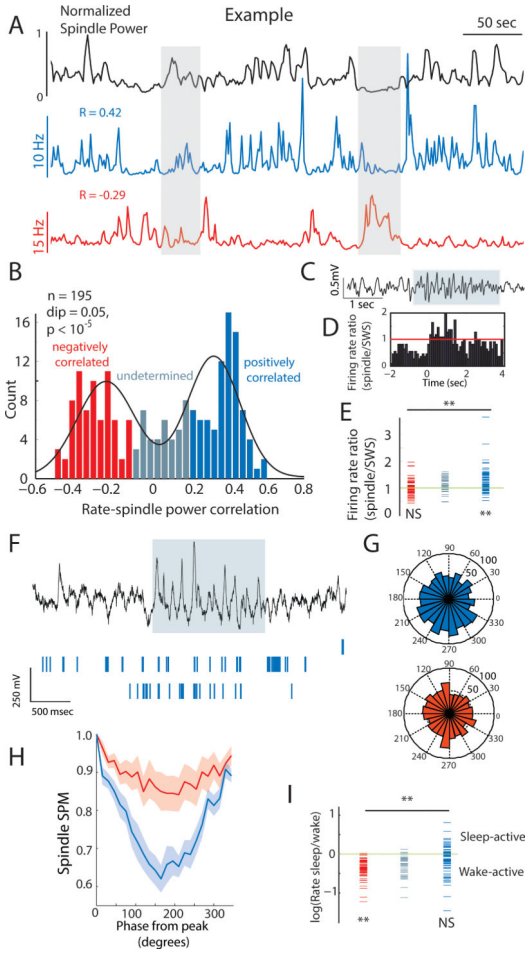

Figure 2. Functional segregation of TRN sub-networks in SWS

(A) Two simultaneously recorded TRN neurons with time-varying firing rates that are positively and negatively correlated with cortical spindle power. **(B)** Bi-modal distribution (Hartigan's dip test, $P < 10^{-5}$) of this correlation across the dataset (n =195 TRN neurons, 7 mice). Grey represents the undetermined group (Methods). **(C)** Example of a detected EEG spindle. **(D)** Peri-event time histogram (PETH) triggered by the onset of cortical spindles showing elevated firing rate of a positively-correlated neuron (determined by analysis similar to **A**) during spindle events. **(E)** This is significant across that population ($P < 10^{-8}$, rank-sum test). **(F)** Two positively correlated (to spindle power, as in **A**) TRN neuronal spike trains in relation to a spindle event. **(G)** Spindle-phase histograms of two TRN neurons (red: negatively-correlated; blue: positively-correlated to spindle power, as in **A**). Note the higher phase locking for the positive-correlated neuron in this example. **(H)** Tendency for higher spindle phase-locking in these neurons as a group (weighted mean ± SEM, rank-sum test: $P = 0.05$ at the point of maximum modulation). **(I)** Negatively-correlated neurons are wake active ($P < 0.01$, rank-sum test), while positively-correlated neurons are state-indifferent ($P< 0.0001$). See also Fig. S2 and table S1.

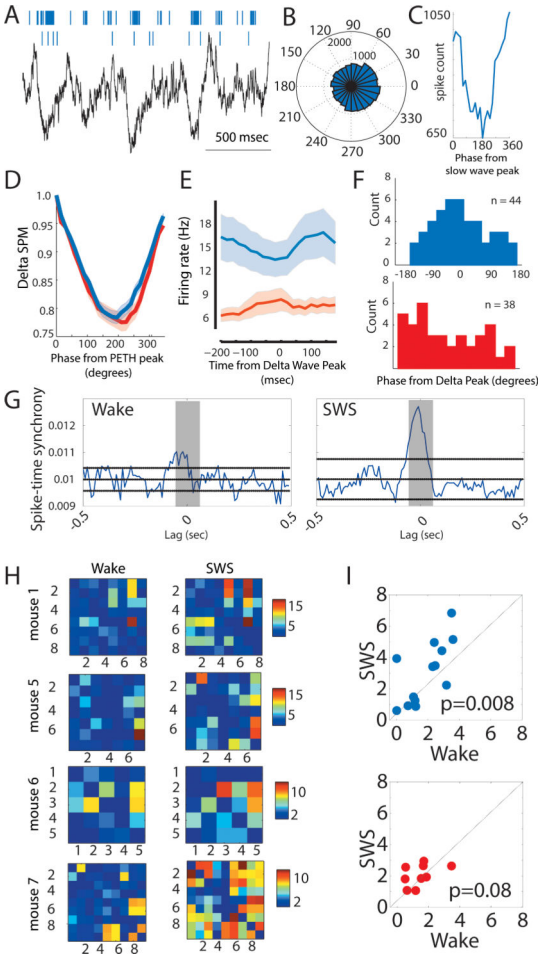

Figure 3. Enhanced synchrony of SC neurons during SWS

(A) During SWS, SC neuronal spiking occurs near cortical slow wave troughs. **(B-C)** Spike delta phase-histogram of a SC neuron shows reduction of firing near the slow wave peaks. **(D)** As a population, SC neurons exhibit comparable delta phase-locking to AC neurons (shaded area denotes the group SEM), shown in the depth of their spike-phase modulation (SPM). **(E)** Delta wave peak-aligned PETH of the SC population (blue trace) shows stronger phase-alignment to cortical delta oscillations than the AC population (red trace). Shaded area is SEM. **(F)** Finding in **E** is further supported by plotting the histogram of the phase values (relative to delta wave peak) at which significantly modulated neurons exhibit minimum spike count. These distributions are significantly different (two-sample Kolmogorov-Smirnov test, $P < 0.03$). Note the peak in the SC neurons histogram, showing that these neurons exhibit little spiking around the peaks of delta oscillations. **(G)** Example of spike-time synchrony between two SC neurons (shaded area: [−50, 50] ms centered at zero lag) showing increased synchrony in SWS. **(H)** Spike-time synchrony (converted to Z-score related to baseline) seen at the ensemble level (examples from four mice). Note the consistent overall elevation of spike-time synchrony among SC units (mouse 1: *n*=8; mouse 5: *n*=7; mouse 6: *n*=5; mouse 7: *n*=9) during SWS compared to wakefulness. **(I)** Group analysis of these ensembles (SC: *n* = 13 ensembles from 4 mice, upper panel; AC: *n* = 9

ensembles from 4 mice, lower panel) shows an increase in SC sub-network synchrony during SWS. Color bar: Z-score. *P*-values: signed-rank test. See also Fig. S3.

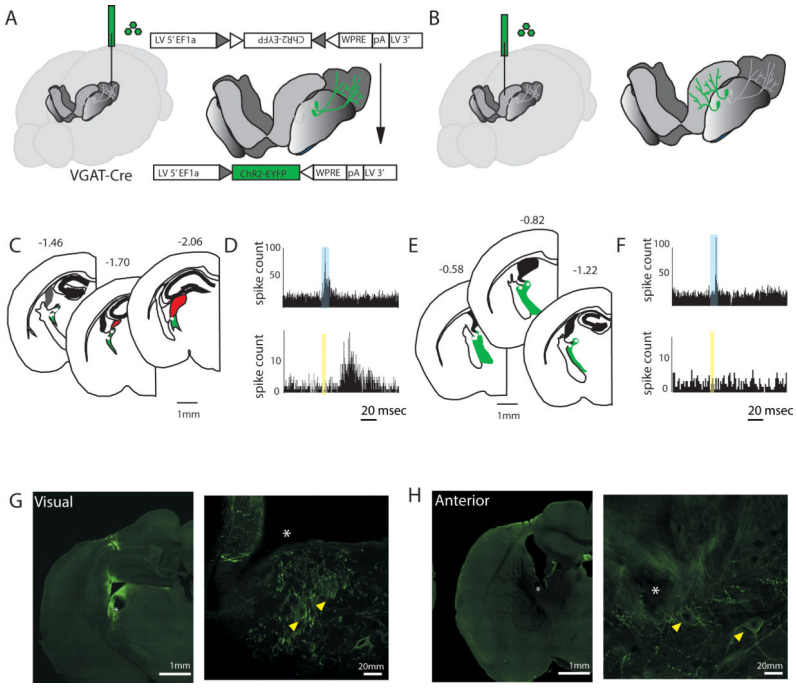

Figure 4. Optogenetic tagging of TRN neurons based on their thalamic targets

(A) Cartoon depiction of optogenetic tagging of visually-connected TRN neurons in mice. A retrograde lentivirus containing a Cre-dependent ChR2-EYFP is injected into the visual thalamus of a VGATCre mouse. 2-4 weeks later, ChR2 is robustly expressed in visually-connected TRN. (**B**) Tagging of anterior complex-connected TRN, similar procedure to **A**. **(C)** Sections showing extracellular recording targets for visually-connected TRN (n = 3 mice). **(D)** Peri-stimulus time histograms (PSTHs) from two visual tagged TRN neurons, showing optogenetic drive with short-latency responses (top) and visual drive with longer latency responses (bottom). **(E-F)** Similar depictions as in **C**-**D**, but for anterior complex-projecting neurons. **(G)** Example brain sections showing electrolytic lesions of electrode tips for visually-connected TRN preparation. Confocal image on the right show electrode tips (white asterisk) near neurons expressing ChR2-EYFP (yellow arrowheads). **(H)** Similar figures to **G**, but for anterior complex-tagged TRN neurons.

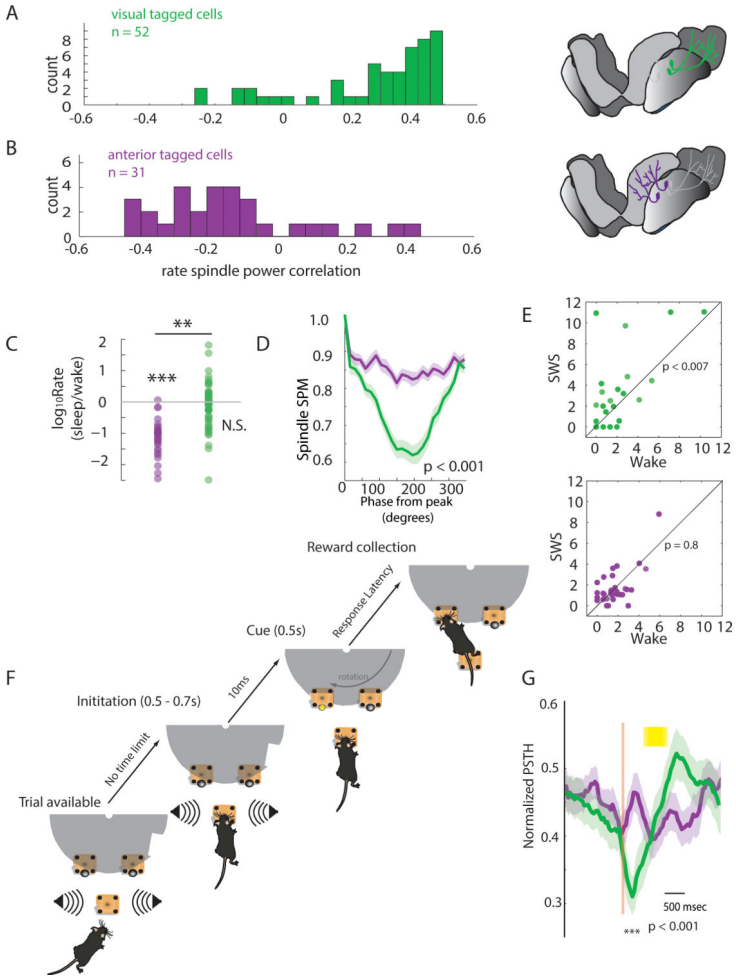

Figure 5. Intact TRN microcircuit dissection connects form to function

(A) Visual tagged neurons are positively correlated to cortical spindle power in SWS ($P<10^{-8}$, signed-rank test), but **(B)** anterior tagged neurons are negatively correlated ($P=0.006$). **(C)** Anterior tagged neurons are wake active, while visual tagged neurons are state-indifferent. **(D)** Visual tagged neurons show stronger phase-locking to spindle oscillations ($P<0.001$, rank-sum test at the trough). **(E)** Visual-, but not anterior-, tagged neurons exhibit enhanced pair-wise spike-time synchrony in SWS (*P*-values: signed-rank test, numbers of axes denote Z-scores). **(F)** Visual detection task design ensures control over psychophysical parameters. The mouse is informed of a new trial by a white noise stimulus emitted from two side speakers. To initiate a trial, the mouse is required to hold its snout in a nose-poke for a period of 0.5-0.7s, ensuring that when the 0.5s stimulus is presented at one of the reward nose-pokes, the head is in the correct orientation to see it. The rotating disk ensures that the reward sites are only available following the stimulus, minimizing impulsive poking behavior. **(G)** Only visual tagged neurons show a reduction in firing rate (group mean ± SEM; $P< 0.001$, rank-sum test) during the attentional window of the visual detection task (yellow bar: stimulus). See also table S2.

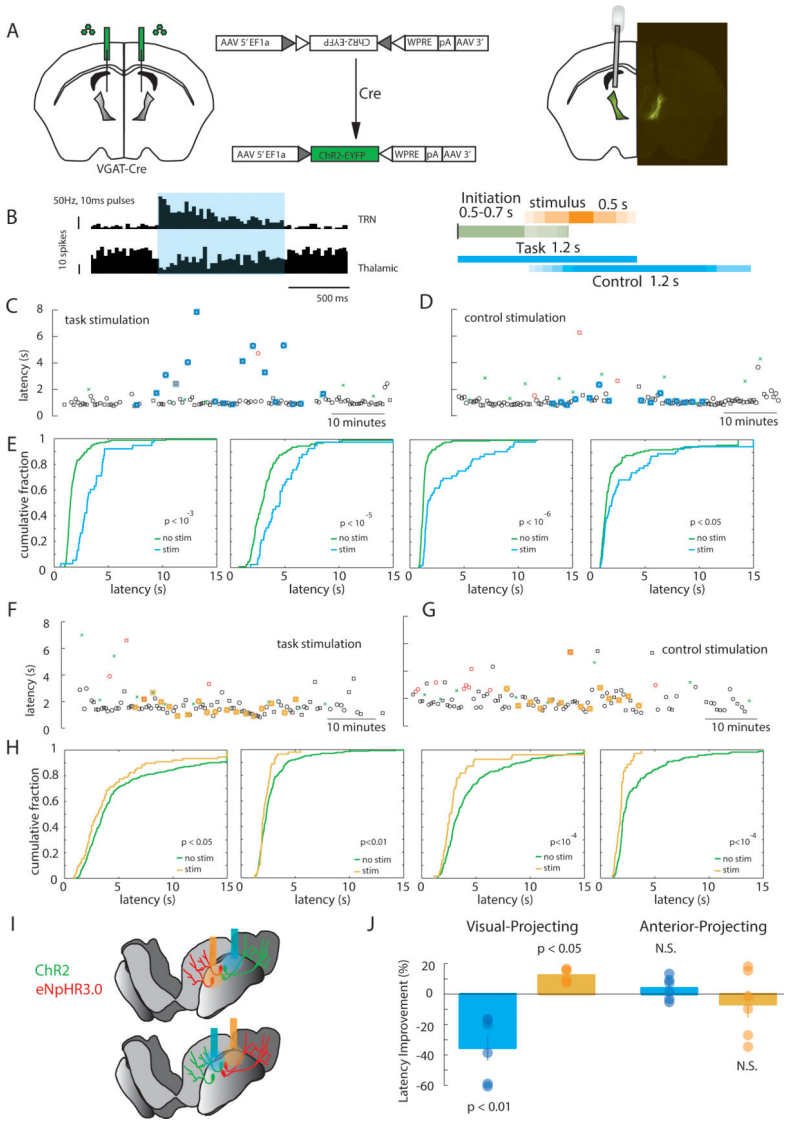

Figure 6. Bi-directional manipulation of cognitive performance by selective TRN targeting

(A) Schematic showing strategy for rendering the TRN optically sensitive. The TRN of a VGAT-Cre mouse is bilaterally injected with an AAV containing a double floxed optogenetic molecule cassette (in this example ChR2-EYFP), which is flipped into frame only in Cre-expressing neurons. Because thalamic relay nuclei are largely devoid of VGAT expressing neurons (except for LGN, which is sufficiently far away from the injection site), ChR2-EYFP expression is limited to the TRN. A similar strategy is used for eNpHR3.0-EYFP experiments **(F-H)**. **(B, left)** Two PSTHs of a TRN unit and a thalamic unit in response to a 50Hz laser stimulus (2ms pulse duration, 1s duration), showing broad elevation in spiking for the TRN unit and broad suppression of spiking in the thalamic unit. **(B, right)** Timeline of optogenetic stimulation regimes in relation to task phases. The same strategy is adopted for optogenetic inhibition. **(C-D)** Examples of a selective TRN stimulation session carried out during all task phases **(C)** or avoiding the initiation phase, but of similar length, 'control stimulation' **(D)**. Note the increased number of long-latency trials

in the task stimulation but not the control one (Black circle: left correct trial, Black square: right correct trial, Red circle: left incorrect trial, Red square: right incorrect trial, Green cross: catch trials, laser trials are highlighted in blue). **(F)** Cumulative distribution of trial latencies (to collect reward) from individual mice, showing diminished performance following TRN activation during the task in all four mice. **(F-G)** Example sessions for eNpHR3.0-mediated TRN inhibition as in **(CD)**. **(H)** Cumulative distribution of trial latencies from individual mice in response to TRN inhibition in the task, showing the opposite behavioral effect to stimulation. **(I)** Set-up for subnetwork specific optogenetic manipulations. **(J)** Optogenetic activation and inhibition of TRN sub-network projecting to visual thalamus diminishes and enhances performance respectively, while similar manipulations of the anterior projecting TRN have an opposite but non-significant effect (n = 6 sessions, 2 mice for each manipulation, P-values: signed-rank test). See also Fig. S6, Movies S1 and S2.

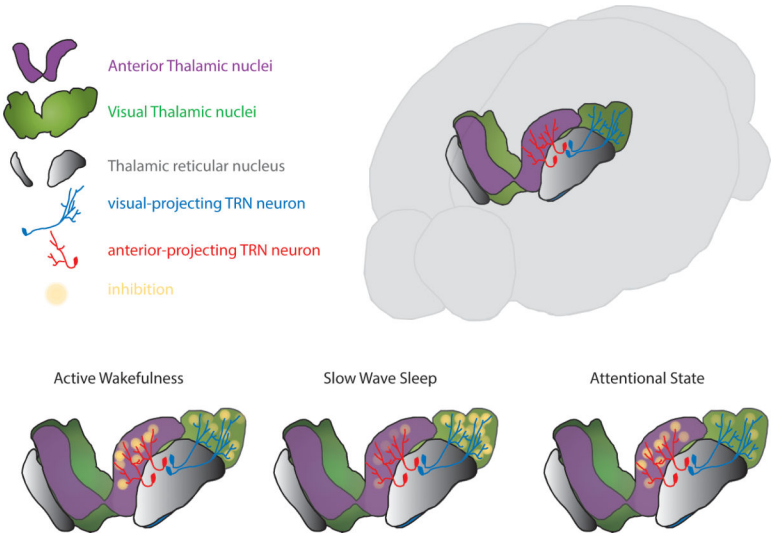

Figure 7. Cartoon depiction of state-dependent thalamic inhibition

During active wakefulness inhibition in sensory and limbic thalamic nuclei is balanced. As the brain transitions to SWS, synchrony among sensory TRN neurons results in enhanced inhibition of sensory thalamic nuclei contributing to gating of external input. The reduction in firing rate of limbic-connected neurons is likely to result in reduced inhibition in limbic thalamus, perhaps facilitating offline processing. During attentional states, sensory neuronal firing rate is reduced, contributing to enhanced sensory thalamic engagement in processing of external stimuli. Although limbic thalamic neurons do not show an overall change in firing rate during these states, individual neurons may participate in shaping limbic processing during these states.